McGlynn, E., Das, R. and Heidari, H. (2020) Encapsulated Magnetoelectric Composites for Wirelessly Powered Brain Implantable Devices. In: 2020 27th IEEE International Conference on Electronics, Circuits and Systems (ICECS), Glasgow, Scotland, 23-25 Nov 2020, ISBN 9781728160443
(doi:10.1109/ICECS49266.2020.9294847)

There may be differences between this version and the published version. You are advised to consult the publisher's version if you wish to cite from it.

http://eprints.gla.ac.uk/223331/

Deposited on 22 September 2020

Enlighten – Research publications by members of the University of Glasgow
http://eprints.gla.ac.uk

Encapsulated Magnetoelectric Composites for Wirelessly Powered Brain Implantable Devices

Eve McGlynn, Rupam Das, Hadi Heidari
Microelectronics Lab (meLAB), James Watt School of Engineering, University of Glasgow, G12 8QQ, UK
Hadi.Heidari@glasgow.ac.uk

***Abstract*—Magnetoelectric devices are readily employed as sensors, actuators, and antennas, but typically exhibit low power output. This paper presents considerations for the viability of magnetoelectric composites for wireless power transfer in neural implantation. This is accomplished herein by studying different types of biocompatible encapsulants for magnetoelectric devices, their impact on the output voltage of the composites, and the rigidity of the materials in the context of tissue damage. Simulation results indicate that a polymer encapsulant, rather than creating a substrate clamping effect, increases the voltage output of the magnetoelectric, which can be further improved by careful polymer selection. These attributes are modelled using the finite element method (FEM) with COMSOL Multiphysics. The addition of a 0.2 mm poly(ethyl acrylate) encapsulating layer increases the piezoelectric voltage to 3.77 V AC output at a magnetic field strength of 200 Oe, as the magnetostrictive layer deforms inside the flexible outer polymer. Comparing voltage conditioning circuits, the output is sufficient for low-voltage neuronal stimulation when employing a simple bridge rectifier which boasts minimal charging time and ripple voltage lower than 1 mV.**

Keywords— Implantable electronics, Magnetoelectric, Polymer composites, Wireless power.

I. Introduction

Implantable medical devices require tens of µW to a few mW which may be provided by an implanted battery with a life span of only a few years. Alternatively, wireless power transfer (WPT) systems employ rigid ceramics for ultrasonic power harvesting, traditional or flexible PCBs for electromagnetic coupling, biocompatible solar panels [1], or metamaterial-based WPT [2]. Magnetoelectric power harvesting presents an opportunity for flexible, miniaturised devices for implantation in future.

Magnetoelectric (ME) coupling creates a change in polarisation (P) of a material for an applied magnetic field (H). The figure of merit for these materials is the ME coefficient, α, in which the value k acts as the "interfacial coupling parameter" for layered composites [3], and defined as

$$\frac{\partial P}{\partial H} = \alpha_{ME} = k_c e^m e, \qquad (1)$$

where, this parameter is in turn multiplied by the piezomagnetic (e^m) and piezoelectric (e) coefficients [4].

Composites, comprised of magnetostrictive and piezoelectric materials, generate considerable power outputs compared to single phase ME, which are severely limited in their output power. Comparatively, composites offer a range of different structures. Piezoelectric rods in a magnetostrictive filler create a robust 1-3 pattern [5] (Fig. 1a). Polymers may be mixed with either particles of magnetostrictive material alone, or also include piezoelectric particles, as shown in Fig. 1b. Layered composites (Fig. 1c) have the lowest current leakage [3] and may be produced from thin films [6]. The geometry significantly impacts the stress in the ME for the same magnetic field (Figs. 1d-f).

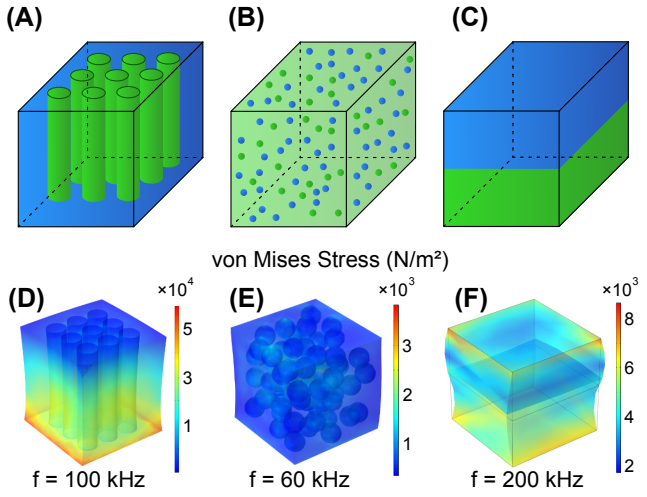

Fig. 1 (A) Piezoelectric 'rods' embedded in magnetostrictive material (1-3 geometry). **(B)** Microcomposite (described herein as 'spheres'), which may take the form of piezoelectric and magnetostrictive particles set in a polymer (0-3). **(C)** Standard laminate ME bilayer, with magnetostrictive on top, piezoelectric below (2-2, described as 'layers'). **(D-F)** von Mises stress of each geometry at resonant frequency, with constant DC magnetic bias and AC amplitude.

ME antennas may be aggressively miniaturised [7], and the impact of ME antenna rigidity is somewhat mitigated by its potentially micrometre scale. However, polymer-based ME devices with useful output voltages are emerging, though they typically cannot compare with more traditional laminate designs. Polymer ME are especially attractive as implants located on or underneath the skull, which must be conformable to reduce damage to the skin or brain surface.

A rigid trilayer with a volume of 1.26 mm^3 is fabricated in [8] with an output power of 42.7 mW, adhering to safety standards for magnetic field exposure. Rod-based ME are modelled in [9] and fabricated in [5]. Particle composites are also modelled in [9], which produced the results expected from literature for the 0-3 (38.4 mV/cmOe) and 1-3 (~1.5 V/cmOe) case, with CFO as the MS material.

One of the most common piezoelectric ceramics is lead zirconate titanate (PZT), which has been proven as biocompatible during acute *in vitro* tests. For the chronic case, elution of PZT in biofluids highlights the high concentration of lead which could cause tissues to become cancerous [10]. To prevent tissue damage, the impact of biocompatible encapsulation on the output voltage is explored, with a

recommendation on the ideal polymer characteristics for increased voltage.

II. Methodology

For this research, the *COMSOL* simulation required three physics solvers: Solid Mechanics, Magnetic Fields, and Electrostatics. The piezoelectric effect is captured by the Multiphysics coupling of Solid Mechanics with Electrostatics, and the magnetostrictive effect is captured by the coupling of Solid Mechanics and Magnetic Fields. Further to this, the setup included a permanent magnet to produce the DC bias; a Helmholtz coil which generates the AC perturbation; and a finite sphere of air.

The permanent magnet was created by applying an Ampère's law condition to the domain with a positive magnetization (M) in the y-axis, to override the original Ampère's law which was automatically applied to all domains. Two multi-turn circular coils were introduced as the Helmholtz coil.

In preparing the three main geometries for the Multiphysics simulations, a JavaScript named *pack-spheres* [11] was used to define the centre points of the particle composite materials, which were subsequently transferred to *SOLIDWORKS,* with the mesh exported to *COMSOL*. To reduce computational time and ensure the minimum mesh element size was suitable for a model built inside an air sphere with a radius of 1 m, each ME cube had sides of 1 cm. Both the spheres and rods had radius 1 mm, while the laminate structure was designed with two layers of equal thickness. In the case of the microcomposite, there were an equal number of magnetostrictive (MS) and piezoelectric (PE) particles set in a piezoelectric polymer.

Simulation parameters for the three ME materials were limited by the availability of key values in the literature. The magnetostrictive material values corresponded to Hitachi 2605SA1 Metglas. However, the B-H curve for this material was not included as a *COMSOL* material: in its place, the curve for 2605S3A-HFA was used. These are both iron-based materials with similar saturation magnetostriction values. The piezoelectric material was chosen as PZT-5H, with PVDF acting as the weakly piezoelectric polymer. The Young's moduli for each of the relevant materials is displayed in Fig. 2, beginning with soft brain tissue.

Key aspects of the simulation setup include specifying a Fixed Constraint boundary condition on the surfaces which should be clamped, creating a Ground and Floating Potential on opposite faces of the piezoelectric layer, and defining the poling direction of the piezoelectric. By default, the poling direction aligns with the z-axis of the model. In contrast, the magnetization in this model was along the y-axis, creating a simple longitudinal-transverse structure.

Initially, the magnetization (M) of the magnet was swept to illustrate the effect of DC bias for each of the geometries. Frequency sweeps were also performed to find the maximum output voltage with optimum DC bias and an AC magnetic field produced by the coil with 100 turns excited by 0.1 A.

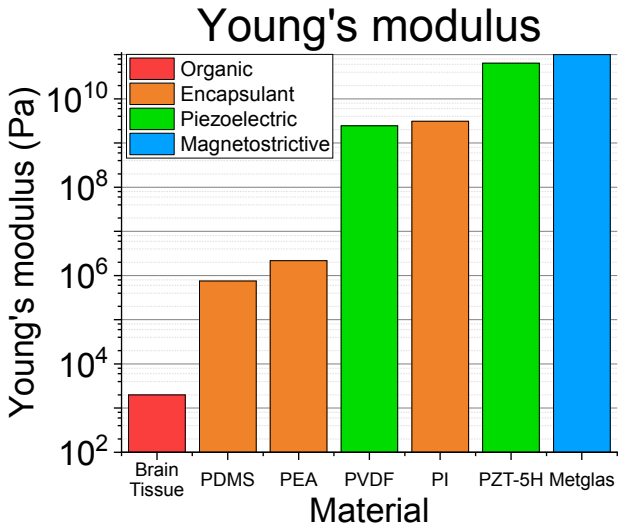

Fig. 2. For all materials presented here, the modulus is at least two orders of magnitude higher than brain tissue. Thin films may go some way to reducing the impact of rigid ME implants on tissue damage. Polydimethylsiloxane (PDMS), poly(ethyl acrylate) (PEA), polyvinylidene (PVDF), polyimide (PI), lead zirconate titanate (PZT-5H).

Subsequently, the AC Helmholtz coil was excited with parameterised current I_0 at the relevant resonant frequency and the voltage output plotted against the applied magnetic field. From this linear graph, the ME coefficient can be calculated by dividing the gradient of the line by the thickness of the piezoelectric layer [12]. A bias field was selected for the bilayer which could produce a resonant peak with the approximate magnitude of 1 V. While this constraint produced a lower value for the DC bias field, improved material selection would yield a magnetostrictive material with a bias field which would conform to medical guidelines.

To investigate the clamping effects of a biocompatible encapsulant on a laminate ME, the thickness of three key biocompatible polymers (PDMS, PI, and PEA) was varied. Further to this, a model encapsulant material was created to investigate the effect of polymer density, Young's modulus and Poisson ratio on the voltage output, as these represented the three variables which changed with each of the three key polymers.

Once the voltage amplitude and phase were gleaned from the PEA-encapsulated example case, the ME voltage was modelled as a standard AC source. When this voltage source was combined with a bridge rectifier and Cockcroft-Walton multiplier, the voltage outputs, ripple voltages and charging periods were compared.

III. Results and Discussion

A. *Comparison of ME Geometries*

It is clear from Fig. 3 that the 1-3 geometry has the largest resonant voltage, and as such would require the lowest bias field for a given output voltage. In the case of 1×10^5 A/m magnetization, it is important to note that the permanent magnet induces a magnetic field with an amplitude of 56.3 Oe, or 4.48 kA/m. Comparatively, the IEEE standard for exposure to magnetic fields above 3 kHz is limited to 163 A/m [13].

An important observation must also be made on the effect of an AC perturbation at the resonant frequency. Despite

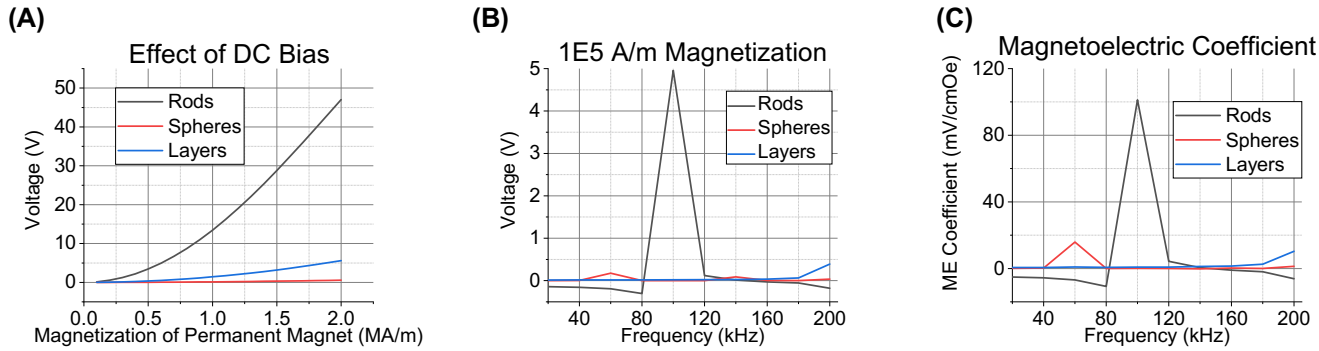

Fig. 3. (A) For the three key geometries, the effect of increasing DC bias indicates that the 1-3 'rods' show the greatest sensitivity, with a significantly higher voltage output compared to the spheres and bilayer. **(B)** With the magnetization of the permanent magnet in the y-direction equal to 1E5 A/m, the resonant peak of each geometry is shown here: 100 kHz, 60 kHz, and 200 kHz for the rods, spheres, and layers respectively. **(C)** ME constant calculated for the same bias field as part (B). The microcomposite or 'spheres' shows an improved value compared to the simple bilayer

having the lowest resonant voltage, the highest peak of the 0-3 geometry is 103.5 times larger than the mean (non-resonant) voltage between 2-200 kHz, whereas the same ratio for the 1-3 geometry equals 37.45. The maximum ME coefficient of the 0-3 geometry is 16 mV/cmOe, less than half of the simulated voltage coefficient as reported by Sun et al. [9] for a CFO-based ME device. This indicates a stronger correlation between the AC field magnitude and output voltage for the composite material when compared to the bilayer. The strong peak at 100 kHz for the 1-3 geometry corresponds to an ME coefficient of 101 mV/cmOe, which is less than 10% of the previously reported value [9].

B. *Polymer Encapsulant Investigation*

The simple bilayer was chosen to perform encapsulation simulations, to reduce computation time. Fig. 4 illustrates the voltage output for a range of encapsulating layer thicknesses (0.2-1 mm), for three biocompatible polymers. In the first instance, the resonant voltage of the encapsulated device was higher than the unencapsulated device (Fig. 4a). The encapsulant also shifted the peak frequency of the ME device down from 200 kHz by a maximum of 40 kHz.

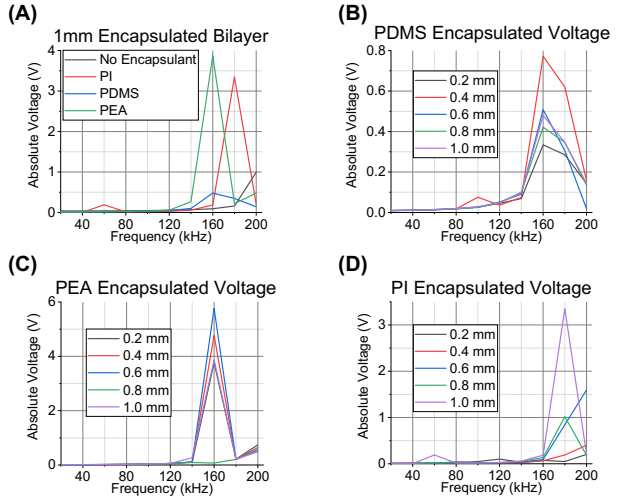

Fig. 4. Frequency sweep for encapsulated ME devices with varying thicknesses. In each case, there is an optimum value: 0.4 mm for PDMS, 0.6 mm for PEA, and 1 mm for PI.

To retain the clamping condition on the top and bottom faces of the ME device, the Fixed Constraint conditions were instead placed on the corresponding faces of the encapsulant. This allowed the magnetostrictive layer to deform within the flexible polymer. As suggested in [14], in which an ME device was coated with parylene-C, the polymer introduces "increased mechanical coupling." Voltage outputs from the model parameterised polymer are shown in Fig. 5.

Table 1 illustrates that for each parameter, PEA aligns closest to the ideal value. This corresponds to the earlier simulations in which the 0.6 mm thick PEA layer voltage output was more than 2 V higher than the maximum PI value (Fig. 4c-d). The significantly lower voltage output for the PDMS-coated ME (Fig. 4b) did not align well with the expected outcome. In addition, the shape of the voltage peak suggested that the maximum voltage for the PDMS-ME would occur between 160 and 180 kHz. For a frequency of 175 kHz, and the 0.8 mm case, the PDMS-ME voltage was 3.77 V. The optimum polymer thickness corresponded to the maximum stress in the bilayer.

TABLE 1. COMPARISON BETWEEN IDEAL AND REAL MATERIAL PROPERTIES.

Polymer	Young's modulus (Pa)	Poisson's ratio (1)	Density (kg/m^3)
Ideal	1E7	0.2	1100
PDMS	7.5E5	0.49	970
PEA	2.18E6	0.3	1210
PI	3.1E9	0.34	1300

C. *Voltage Rectification and Smoothing*

The AC voltage output of an ME device must be rectified and smoothed for the purposes of neuronal stimulation. Low voltage devices deliver 1-4 V, while 5-10 V is classed as high voltage stimulation [15]. As such, the example case for a PEA-coated (0.2 mm encapsulant thickness) bilayer was modelled in *PSpice* as a 3.77 V 160 kHz AC voltage source (see Fig. 6). Using a bridge rectifier and smoothing capacitor, this was reduced to 2.94 V DC with a ripple voltage of 0.90 mV. By contrast, a single-stage Cockcroft-Walton voltage multiplier with the same capacitor values delivered 3.80 V with a ripple voltage of 56 mV.

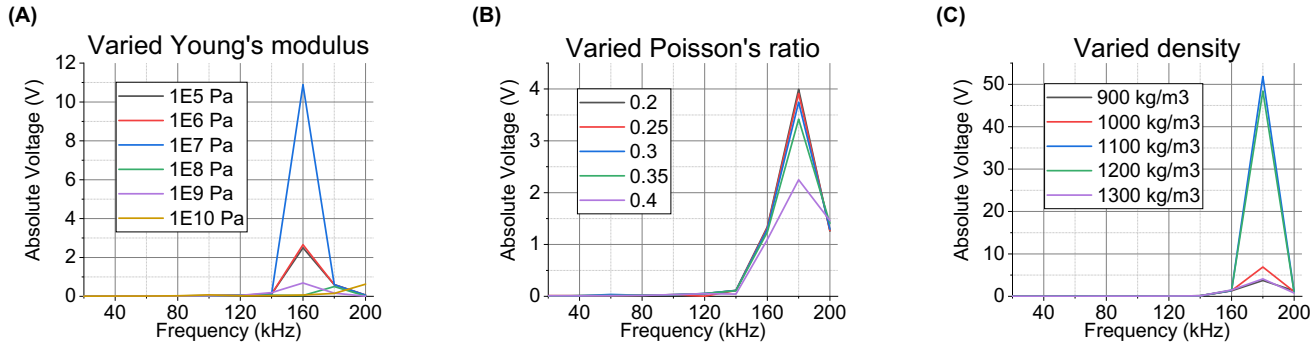

Fig. 5. Parameterised values for the Young's modulus, Poisson's ratio, and density illustrated a clear improvement in the output voltage for values summarised in Table 1. While one of these parameters was swept, the other two values were kept constant at E = 1E7 Pa, ν = 0.3, and ρ = 900 kg/m^3. For each simulation, the solver mesh, bilayer setup, and layer thickness were unchanged.

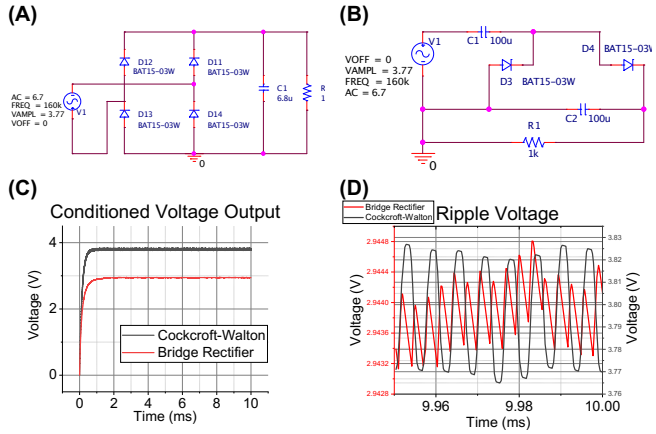

Fig. 6. (A) Bridge rectifier and smoothing capacitor. **(B)** Single-stage Cockcroft-Walton voltage multiplier. **(C)** Output showing maximum voltage and charging period. **(D)** Ripple voltage around 1 mV for both circuits. Diode selection based on [16].

For comparable charging times, the bridge rectifier has a much lower ripple voltage, and a reduced voltage output. Increasing the capacitor size for the Cockcroft-Walton circuit would not only increase the charging time, but the physical size of the components. Since both voltage outputs are suitable for low-voltage stimulation, the rectifier is preferable.

IV. Conclusion

The impact of geometry and encapsulation on an ME device was explored for the purposes of ascertaining their suitability for implantable neuronal stimulation. Despite the rigid materials employed in the 1-3 geometry, it has the highest voltage output for a reduced bias field. Subsequently, it is shown that polymer coating may be used to maximise the deformation of the MS and increase the output voltage, while PEA is the superior choice in this case. This represents an important opportunity to improve the performance of ME composites. Finally, a bridge rectifier would be well suited to low-voltage neuronal stimulation, with reduced ripple and charging time compared to the Cockcroft-Walton multiplier.

References

[1] R. Das and F. Moradi, "Biointegrated and Wirelessly Powered Implantable Brain Devices: A Review," *IEEE Transactions on Biomedical Circuits and Systems,* pp. 1-13, 2020.

[2] R. Das and H. Heidari, "A Self-tracked High-dielectric Wireless Power Transfer System for Neural Implants," in *2019 26th IEEE International Conference on Electronics, Circuits and Systems (ICECS)*, 2019: IEEE, pp. 111-112.

[3] M. Bichurin, V. Petrov, and G. Srinivasan, "Theory of low-frequency magnetoelectric coupling in magnetostrictive-piezoelectric bilayers," *Physical Review B,* vol. 68, no. 5, p. 054402, 2003.

[4] S. Lanceros-Méndez and P. Martins, *Magnetoelectric Polymer-based Composites: Fundamentals and Applications*. John Wiley & Sons, 2017.

[5] K. Lam, C. Lo, and H. L. Chan, "Frequency response of magnetoelectric 1–3-type composites," *Journal of Applied Physics,* vol. 107, no. 9, p. 093901, 2010.

[6] S. Zuo *et al.*, "Ultrasensitive Magnetoelectric Sensing System for pico-Tesla MagnetoMyoGraphy," *IEEE Transactions on Biomedical Circuits and Systems,* 2020.

[7] T. Nan *et al.*, "Acoustically actuated ultra-compact NEMS magnetoelectric antennas," *Nat Commun,* vol. 8, no. 296, pp. 1-8, 2017.

[8] T. Rupp, B. D. Truong, S. Williams, and S. Roundy, "Magnetoelectric Transducer Designs for Use as Wireless Power Receivers in Wearable and Implantable Applications," *Materials,* vol. 12, no. 3, p. 512, 2019.

[9] T. Sun, L. Sun, Z. Yong, H. L. Chan, and Y. Wang, "Estimation of the magnetoelectric coefficient of a piezoelectric-magnetostrictive composite via finite element analysis," *Journal of Applied Physics,* vol. 114, no. 2, p. 027012, 2013.

[10] C. K. Jeong *et al.*, "Comprehensive biocompatibility of nontoxic and high-output flexible energy harvester using lead-free piezoceramic thin film," *APL Materials,* vol. 5, no. 7, p. 074102, 2017.

[11] *pack-spheres*. (2019). GitHub. [Online]. Available: https://github.com/mattdesl/pack-spheres

[12] M. Vopson, Y. Fetisov, G. Caruntu, and G. Srinivasan, "Measurement techniques of the magneto-electric coupling in multiferroics," *Materials,* vol. 10, no. 8, p. 963, 2017.

[13] IEEE International Committee on Electromagnetic Safety, "IEEE Standard for Safety Levels with Respect to Human Exposure to Electric, Magnetic, and Electromagnetic Fields, 0 Hz to 300 GHz," *IEEE Std C95.1-2019,* pp. 1-312, 2019.

[14] A. Singer *et al.*, "Magnetoelectric materials for miniature, wireless neural stimulation at therapeutic frequencies," *Neuron,* 2020.

[15] R. Ramasubbu, S. Lang, and Z. H. Kiss, "Dosing of electrical parameters in Deep Brain Stimulation (DBS) for intractable depression: a review of clinical studies," *Front Psychi,* vol. 9, p. 302, 2018.

[16] A. Lasheras *et al.*, "Energy harvesting device based on a metallic glass/PVDF magnetoelectric laminated composite "*Smart Materials and Structures,* 2015.